

iScience, Volume 25

Supplemental information

**An adipose IncRAP2-Igf2bp2 complex enhances
adipogenesis and energy expenditure by
stabilizing target mRNAs**

Juan R. Alvarez-Dominguez, Sally Winther, Jacob B. Hansen, Harvey F. Lodish, and Marko Knoll

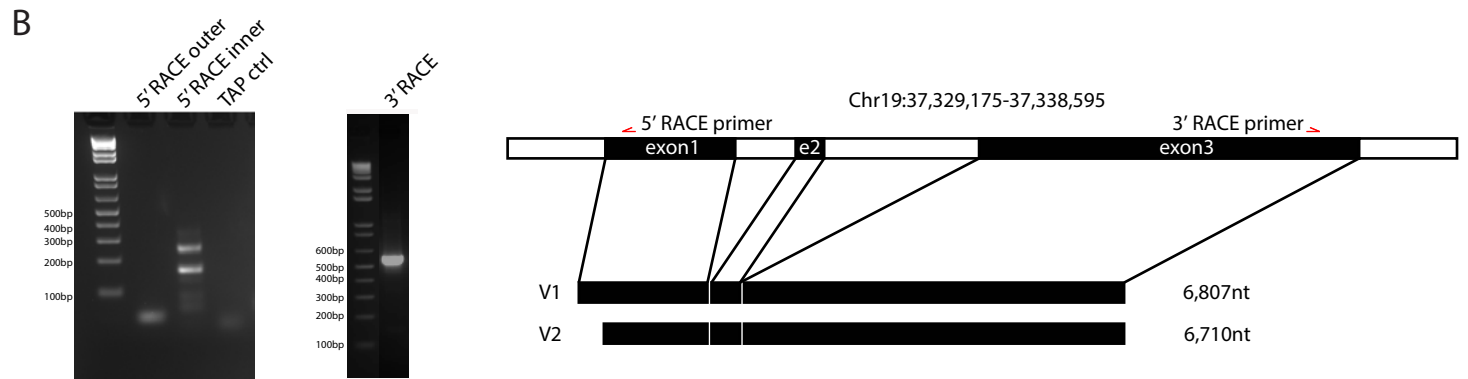
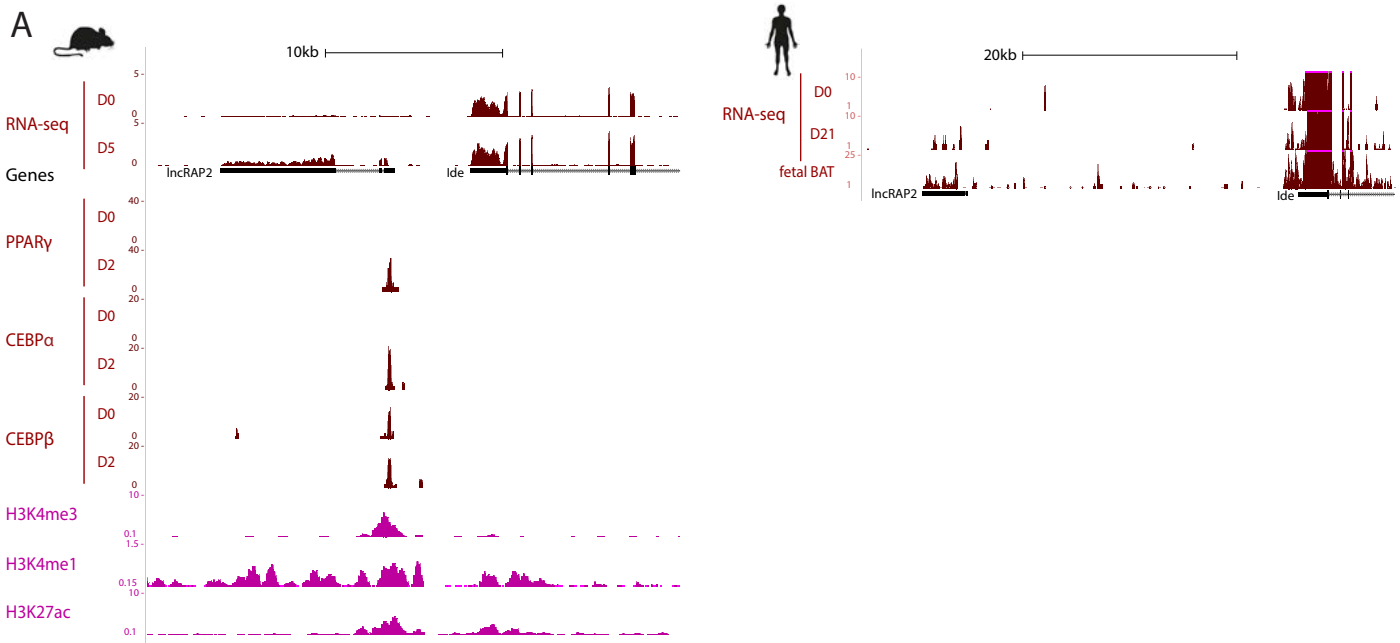


Figure S1. lncRAP2 is a conserved cytoplasmic RNA required for adipogenesis. Related to Figure 1.

(A) lncRAP2 (transcription right-to-left) structure, expression, and regulation in brown adipocytes. Tracks show signal from sequencing studies of primary brown adipocytes from mouse (A) and human (Ding et al., 2018) (B).

(B) Rapid amplification of cDNA ends (RACE) delineates the lncRAP2 transcript. The genomic locus, spliced transcript variants (V1 and V2), RACE primers, and the amplified 5' and 3' end fragments sequenced are shown.

Figure S2. lncRAP2 forms a complex with proteins that regulate mRNA stability and translation. Related to Figure 2.

- (A) lncRAP2 is expressed at comparable levels in subcutaneous white adipose tissue (scWAT), upon *in vitro* differentiation of scWAT preadipocytes, and upon *in vitro* differentiation of 3T3-L1 preadipocytes.
- (B) Specific and reproducible enrichment of spliced lncRAP2 by antisense purification. Tracks show signal from RNA interactome analysis by sequencing (RIA-seq) studies of differentiated white adipocytes. Locations of lncRAP2 exon- and intron-targeting antisense probe pools are shown below.
- (C) lncRAP2 does not directly bind other RNAs. A minority of RIA-seq peaks are common to both lncRAP2 exon-targeting probe pools, and show poor enrichment or concordance between the probe pools, other than the peaks from capturing lncRAP2 itself.
- (D) lncRAP2 antisense purification retrieves rich protein analytes compared to controls. The specific enrichment of protein analytes in differentiated 3T3-L1 adipocytes recovered by Silver stain of captured proteins before mass spectrometry analysis is shown.
- (E) Specific native immunoprecipitation of Igf2bp2 (highlighted) in primary mouse white adipocytes. Western blot of captured proteins from an aliquot after pulldown with an Igf2bp2-specific antibody.
- (F) *Igf2bp2* expression in select tissues. Relative expression in different organs and tissues from mouse (Alvarez-Dominguez et al., 2015) (top) and human (Uhlen et al., 2015) (bottom) is shown. Human adipose tissue pools samples from subcutaneous and visceral depots.
- (G) *Igf2bp2* expression during an *in vitro* differentiation timecourse of mouse inguinal white adipose tissue and interscapular brown adipose tissue preadipocytes (left) and human subcutaneous adipose tissue and fetal interscapular brown adipose tissue preadipocytes (Ding et al., 2018) (right).
- (H) Igf2bp2 protein levels during *in vitro* differentiation of mouse white or brown preadipocytes. Western blots for the indicated proteins are shown.

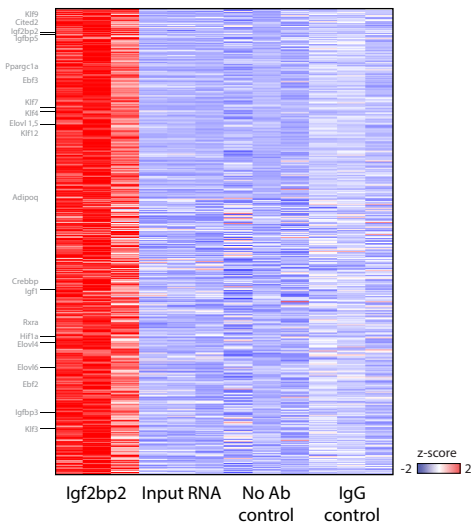
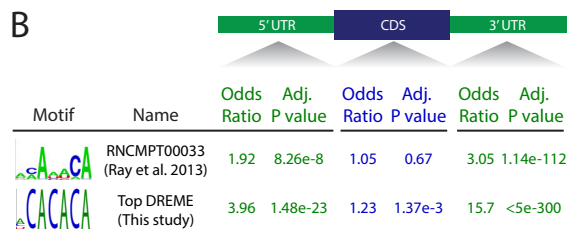
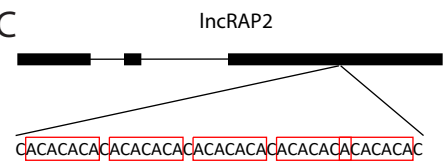
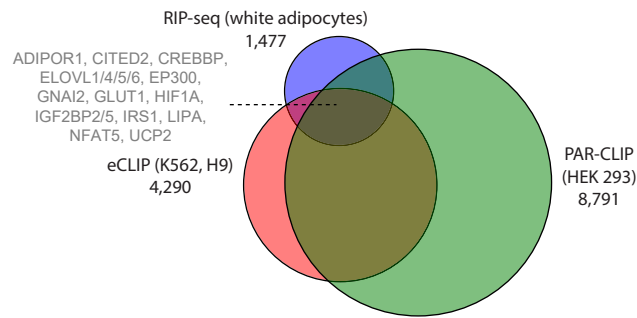
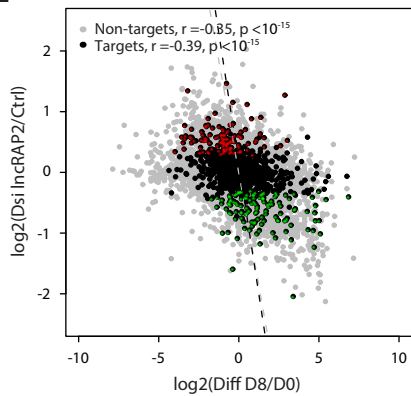
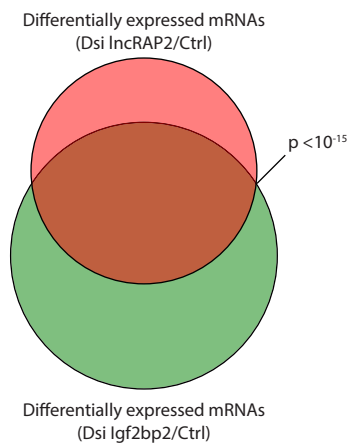
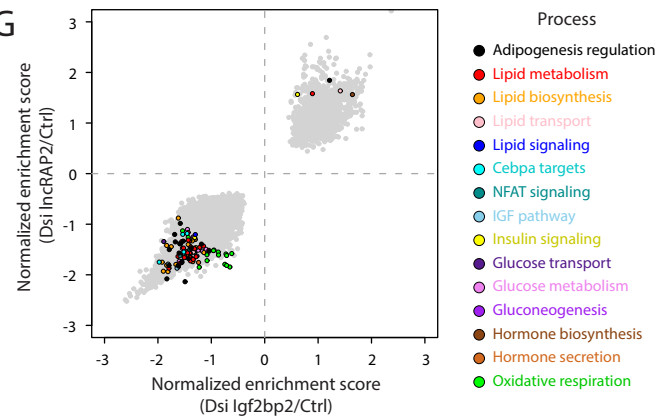
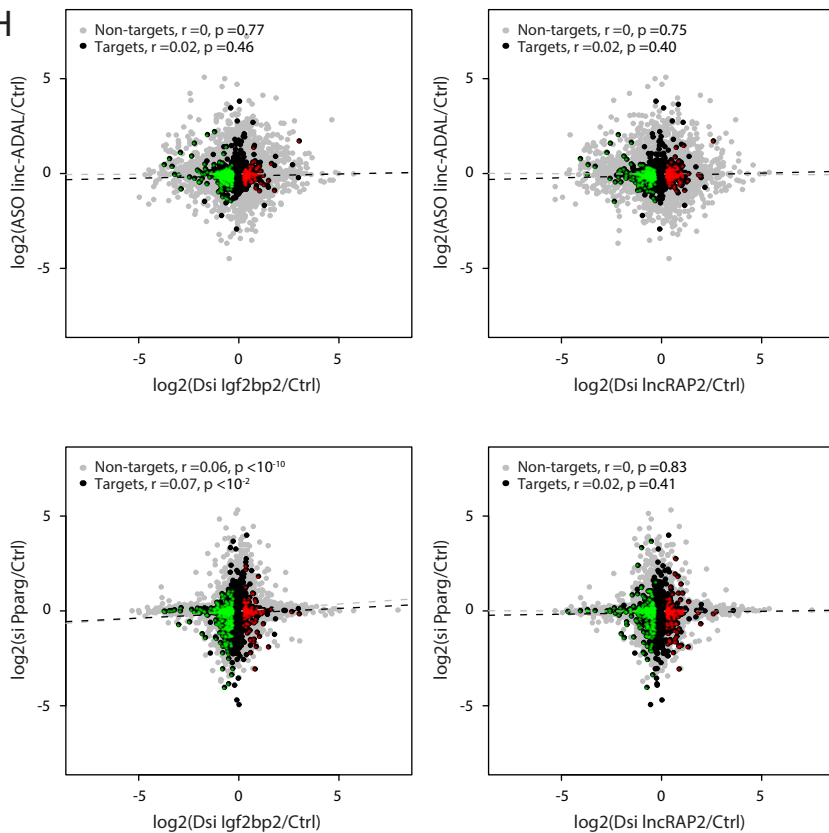
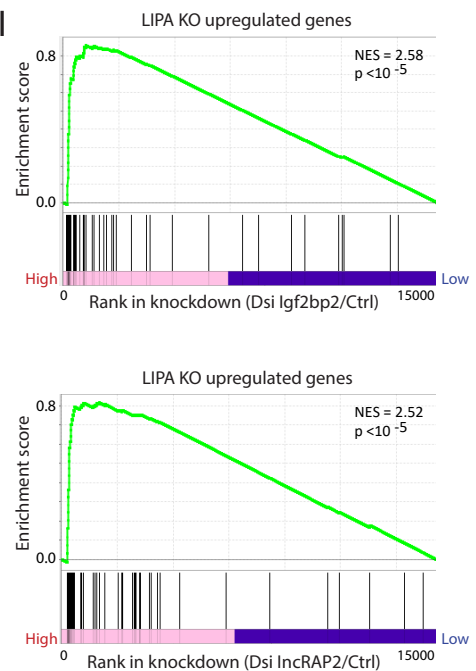
A Igf2bp2 targets in white adipocytes**B****C****D****E****F****G****H****I**

Figure S3. lncRAP2-Igf2bp2 target transcripts of metabolic effectors to potentiate energy expenditure. Related to Figure 3.

(A) Igf2bp2 selectively binds mRNAs encoding adipogenic regulators and effectors. Enrichment of RNAs in native Igf2bp2 or control immunoprecipitates (n=3 replicates each) in mouse white adipocytes.

(B) Igf2bp2 targets enrich for the known Igf2bp2 binding motif predominantly within their 3'UTRs. Computational analysis of short motifs and their relative enrichment within the 5'UTR, coding sequence, and 3'UTR regions of transcripts bound by Igf2bp2 in mouse white adipocytes. The top DREME (Bailey, 2011) motif identified (bottom) and the experimentally inferred Igf2bp2 binding motif (Ray et al., 2013) (top) are compared.

(C) lncRAP2 harbors multiple Igf2bp2 binding motif instances. The sequence of five intact motifs (two are overlapping) and their location within the lncRAP2 transcript are shown.

(D) Most Igf2bp2 targets in mouse white adipocytes also copurify with Igf2bp2 in human cells. Overlap between 1,477 targets identified by RNA immunoprecipitation sequencing (RIP-seq) in mouse white adipocytes that have human homologs, those identified by enhanced crosslinking and immunoprecipitation (eCLIP) in human embryonic stem (H9) (Conway et al., 2016) and in erythroleukemia (K562) cells (Van Nostrand et al., 2016), and those identified by photoactivatable ribonucleoside-enhanced crosslinking and immunoprecipitation (PAR-CLIP) in human embryonic kidney (HEK 293) cells (Hafner et al., 2010). Common adipogenic regulator and effector targets identified by all three methods are highlighted.

(E) The induction/suppression of Igf2bp2 RNA targets with adipogenesis is reversed in lncRAP2-depleted cells. RNA changes for Igf2bp2 targets (black circles) and non-targets (gray circles) upon *in vitro* differentiation of lncRAP2-depleted vs. untreated mouse scWAT preadipocytes is shown. Genes significantly ($p < 0.05$) upregulated (red) or downregulated (green) upon lncRAP2 depletion are highlighted.

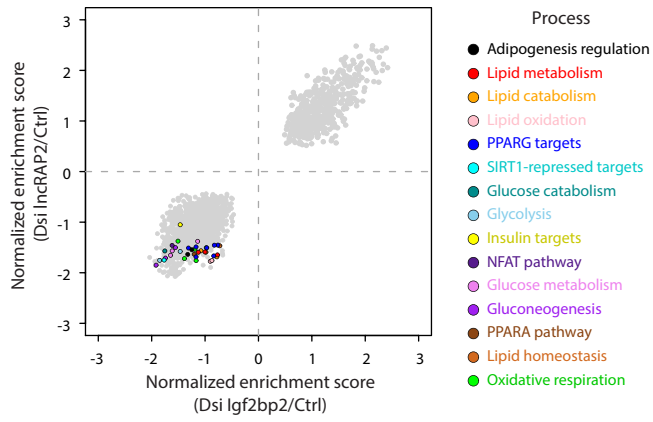
(F) Significant overlap ($p < 10^{-15}$, hypergeometric test) between mRNAs that are differentially expressed ($p < 0.05$, t-test) after lncRAP2 depletion (top) and after *Igf2bp2* depletion (bottom).

(G) lncRAP2/*Igf2bp2* depletion cause selective destabilization of transcripts encoding mediators of energy metabolism. Gene set enrichment analysis highlighting significant ($p < 0.05$) biological processes upon *Igf2bp2* vs. lncRAP2 depletion.

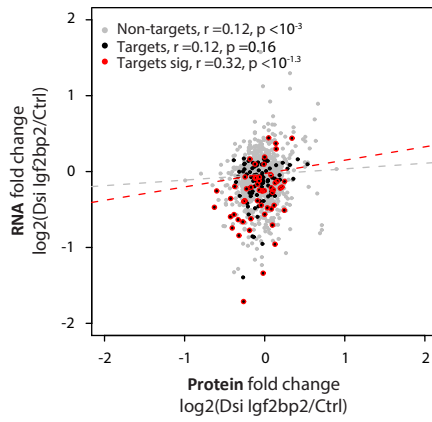
(H) No correlation between transcriptome-wide effects of depleting lncRAP2 or Igf2bp2 with those of depleting Ppar γ or linc-ADAL (lincRNA for adipogenesis and lipogenesis). Shown are RNA changes for Igf2bp2/lncRAP2 targets (black circles) and non-targets (gray circles) upon antisense oligonucleotide (ASO)-mediated depletion of linc-ADAL or siRNA-mediated depletion of Pparg in mature white adipocytes (Schupp et al., 2009; Zhang et al., 2018). Genes significantly ($p < 0.05$) upregulated (red) or downregulated (green) upon Igf2bp2 or lncRAP2 depletion are highlighted.

(I) Gene set enrichment analysis reveals significant overlap between the lncRAP2 and *Igf2bp2* depletion gene signatures and that of genes up-regulated (≥ 2 fold-change) at 6 months of age in lungs from lysosomal acid lipase gene knockout mice (Lian et al., 2005). NES, normalized enrichment score.

A



B



C

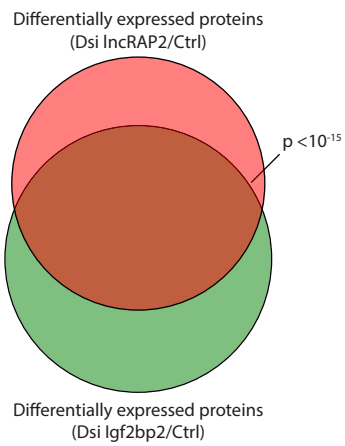


Figure S4. lncRAP2-Igf2bp2 predominantly tune the levels of target mRNAs. Related to Figure 3.

(A) lncRAP2 and *Igf2bp2* depletion cause coordinate reduction in levels of key energy metabolism effector proteins. Gene set enrichment analysis highlighting significant ($p < 0.05$) biological processes upon *Igf2bp2* vs. lncRAP2 depletion in mature white adipocytes.

(B) Coordinate RNA and protein changes upon *Igf2bp2* depletion. Global protein vs. RNA changes upon *Igf2bp2* depletion in mature white adipocytes, highlighting *Igf2bp2* targets with protein changes that are significant after *Igf2bp2* depletion ($p < 0.05$, red) or not (black).

(C) Significant overlap ($p < 10^{-15}$, hypergeometric test) between proteins that are differentially expressed ($p < 0.05$, t-test) after lncRAP2 depletion (top) and after *Igf2bp2* depletion (bottom).

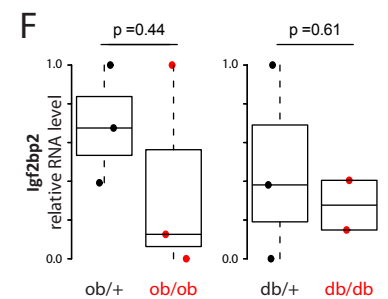
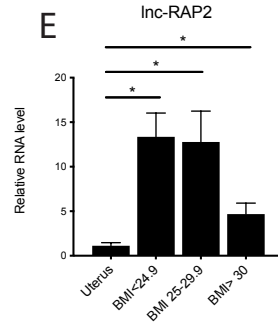
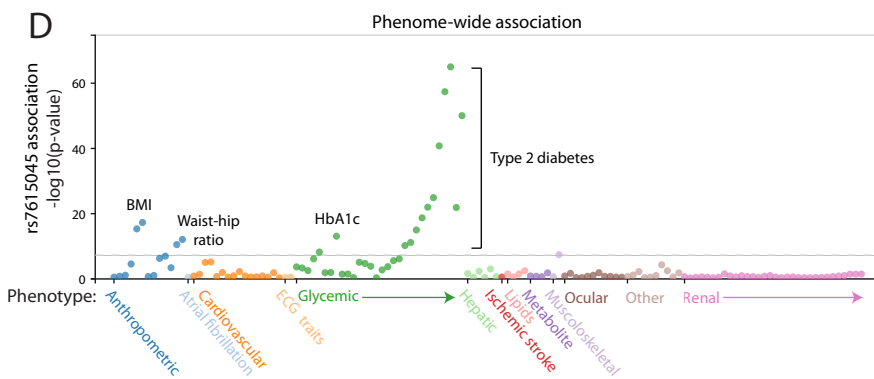
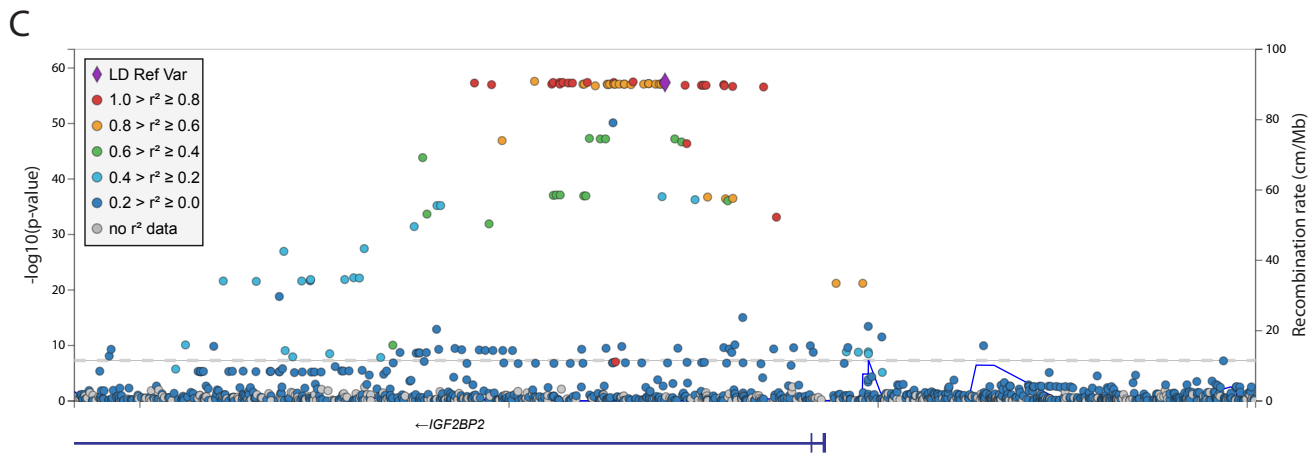
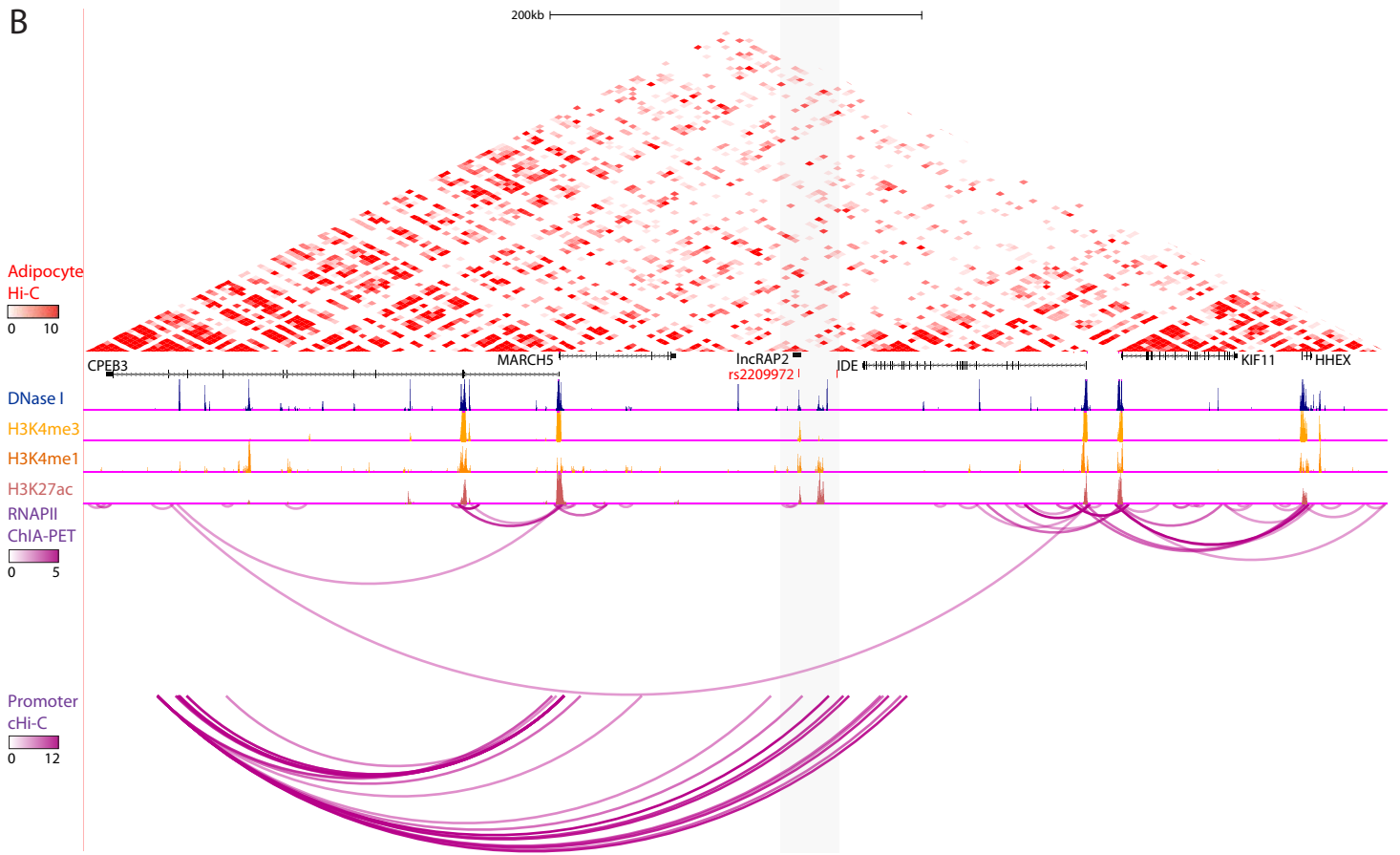
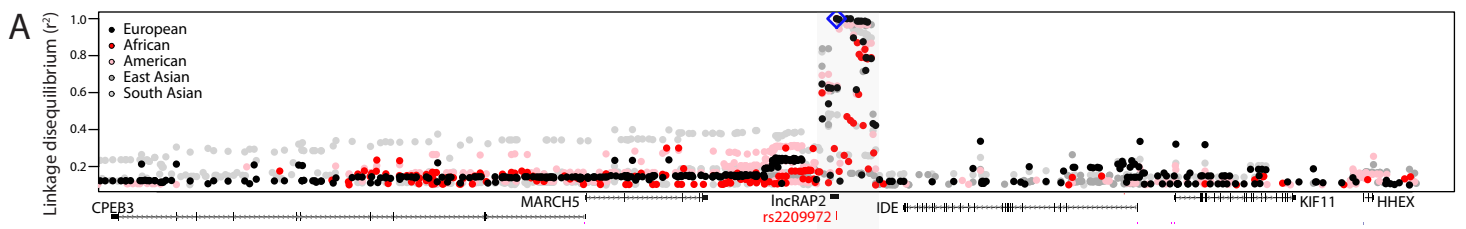


Figure S5. lncRAP2-Igf2bp2 genetic and expression variability are associated with obesity-linked diabetes risk. Related to Figure 4.

(A) Human rs2209972 is in strong linkage disequilibrium with genetic variants within lncRAP2 but no other loci within 500kb. Linkage disequilibrium with rs2209972 (diamond) based on 1000 Genomes (Genomes Project et al., 2015) data for the indicated populations.

(B) Human rs2209972 maps to a lncRAP2 interaction domain. Heatmap displays human white adipocyte chromatin conformation by Hi-C (Paulsen et al., 2019). Tracks below display open chromatin and histone mark sequencing studies, and chromatin interactions involving RNA polymerase II or captured promoter regions (Table S4).

(C) Regional association with type 2 diabetes at the IGF2BP2 locus. Significance of association between genetic variants surrounding the IGF2BP2 transcription start site and type 2 diabetes in 898,130 European-descent individuals (Mahajan et al., 2018). Variants are colored based on 1000 Genomes All samples (Genomes Project et al., 2015) linkage disequilibrium with rs7615045 (diamond).

(D) IGF2BP2 rs7615045 is specifically associated with body mass, glycated hemoglobin (HbA1c), and type 2 diabetes. Phenome-wide association results between rs7615045 and 317 phenotypes across 16,278,030 individuals of various ancestries from the Type 2 Diabetes Knowledge Portal (<http://www.type2diabetesgenetics.org/variantInfo/variantInfo/rs7615045>). Only significant ($p < 0.05$) associations are shown.

(E) Adipose lncRAP2 is reduced with obesity. Shown are relative lncRAP2 levels (normalized to uterus, left) in adipose tissue samples pooled from patients with different body mass index (BMI) (Table S3).

(F) *Igf2bp2* is suppressed during diabetes onset and progression. *Igf2bp2* levels in visceral adipose tissue from leptin-deficient (*ob/ob*) and leptin receptor-deficient (*db/db*) 9-10 week-old mice (Wang et al., 2012a).

Table S1: Primer and DsiRNA sequences related to Key Results Table

Primer mouse	forward 5' - 3'	reverse 5' - 3'	Source	Identifier
lnc-RAP-2	GGTCCTTAGGCAGAGTCTTG	TCCATGGAGCACAATAGCTG	doi: 10.1073/pnas.1222643110.	IDT
18S	GTAACCCCGTTGAACCCCAAT	CCATCCAATCGGTAGTAGC	doi: 10.1038/ncb2286.	IDT
47s pre rRNA	CTCCTGTCTGTGGTGTCCAA	TGATACGGGCAGACACAGAA	This paper	IDT
AdipoQ	CGATTGTCAGTGGATCTGACG	CAACAGTAGCATCCTGAGCCCT	doi: 10.1038/ncb2286.	IDT
Cebpalpha	TGCGCAAGAGCCGAGATAAA	CCTTCTGTTGCGTCTCCACG	doi: 10.1038/ncb2286.	IDT
Fabp4	ACAAGCTGGTGGTGGAAATGTG	CCTTTGGCTCATGCCCTTT	doi: 10.1038/ncb2286.	IDT
Ppargamma	GTGCCAGTTTCGATCCGTAGA	GGCCAGCATCGTGTAGATGA	doi: 10.1038/ncb2286.	IDT
Glut4	CTGTCGCTGGTTTCTCCAAC	CCCATAGCATCCGCAACATA	doi: 10.1038/ncb2286.	IDT
lnc-FIRRE	AGCCATTTTGAAGCAGGGA	CTCTGAAGGGTCAGGTGATG	doi: 10.1038/nsmb.2764.	IDT
IGF2bp2	GACTACCCCGACCAGAACATG	GAGGCGGGATGTTCCGAATC	This paper	IDT
IGF2	GTGCTGCATCGCTGCTTAC	ACGTCCTCTCGGACTTGG	This paper	IDT
Pgc1alpha	CCCTGCCATTGTAAAGACC	TGCTGCTGTTCTGTTTTTC	doi: 10.1038/ncb2286.	IDT
Cidea	TGCTCTTCTGTATCGCCCAAGT	GCCGTGTAAAGGAATCTGCTG	doi: 10.1038/ncb2286.	IDT
Elov13	TTCTCACGCGGGTTAAAAATGG	GAGCAACAGATAGACGACCAC	This paper	IDT
5'RACE g.s. RAP2 5'	TTTCGCTTTCACAAACAATC	0	This paper	IDT
5'RACE g.s. RAP2 inner	TCCACATTGCAATTCCTTTCT	0	This paper	IDT
5'RACE g.s. RAP2 outer	TGGACTTCAGGGCCTCAGT	0	This paper	IDT
3'RACE g.s. RAP2 outer	TGGAGTAAGGAATTTGCACCT	0	This paper	IDT
3'RACE g.s. RAP2 inner	CCTCCTCCTTTTCTCTTCC	0	This paper	IDT
M13	GTAAAACGACGGCCAG	CAGGAAACAGCTATGAC	Thermo Fisher Scientific	K4575 J10
0	0	0	0	0
Primer human	forward 5' - 3'	reverse 5' - 3'	Source	Identifier

huIncRAP-2	TAAATACTGCAGGCGAAG GAC	CCTTCTACCCGCGTCATCA	This paper	IDT
human18S	GTAACCCGTTGAACCCCA TT	CCATCCAATCGGTAGTAGC G	This paper	IDT
0	0	0	0	0
DsiRNAs	forward 5'-3'	reverse 5'-3'	Source	Identifier
DsiRNA IncRAP-2 #1	CTGCATGGATGTTTTGTTT AGTCAA	AACTGATTTGTTTTGTAGGT ACGTCCT	This paper	IDT
DsiRNA IncRAP-2 #2	CTTCTACAAGAAATCAGA AACAGTA	ATGACAAAGACTAAAGAAC ATCTTCAG	This paper	IDT
DsiRNA Igf2bp2 #1	AAGCAGTGCTCTGAATAT CATACCA	TGGTATGATATTCAGAGCA CTGCTTTG	mm.Ri.Igf2bp2.13. 1	IDT
DsiRNA Igf2bp2 #2	AAGAGGCAAAGCTAGCT ATTGAGAA	TTCTCAATAGCTAGCTTTGC CTCTTCT	mm.Ri.Igf2bp2.13. 2	IDT